ARID ZONE JOURNAL OF ENGINEERING, TECHNOLOGY & ENVIRONMENT
AZOJETE March 2024. Vol. 20(1):295-304
Published by the Faculty of Engineering, University of Maiduguri, Maiduguri, Nigeria.
Print ISSN: 1596-2490, Electronic ISSN: 2545-5818
www.azojete.com.ng

PERFORMANCE EVALUATION OF A HYBRID SOLAR-WIND POWER SYSTEM FOR HEIPANG COMMUNITY LOAD DEMAND

I. B. Maren[1]*, A. B. Adisa[2], H. Dandakouta[3] and R. I. Ejilah[3]

[1]Department of Mechanical Engineering, University of Jos, Plateau State, Nigeria
[2]Department of Mechanical and Production Engineering, Abubakar Tafawa Balewa University, Bauchi State, Nigeria
[3]Department of Automobile Engineering Abubakar Tafawa Balewa University, Bauchi State, Nigeria.

**Corresponding author's email address: mareni@unijos.edu.ng*

ARTICLE INFORMATION

Submitted 27 September, 2023
Revised 26 December, 2023
Accepted 25 February, 2024

Keywords:
Load Sharing Strategy (LSS)
Hybrid system
Simulation
Capacity factor
Design

ABSTRACT

The electricity generation capacity of Nigeria, which is predominately fossil-based and unsustainable, is far below the energy needs of its growing population and industrial demand. There is a need therefore to increase the level of renewable energy in the energy mix to reduce the adverse effect of fossil fuels on the environment and enhance access to electricity. Assessing the performance of renewable energy systems in a location is a prerequisite for embarking on the technology. In this paper, 10-year average minimum solar radiation and wind speed data of the Heipang community of Barkin-Ladi LGA of Plateau State and load sharing strategy design approach were used to design a hybrid solar wind power system to meet the load demand of the Heipang community. MATLAB codes were written to simulate the designed hybrid solar-wind power system to assess its performance over the year against the given load demand profile using one-year hourly global solar radiation, wind speed, and ambient temperature data. Results show that for a load demand of 158.32 kW and a daily energy demand of 710.59 kWh/day, with two-day autonomy, it will require 283 units of 300W capacity solar panels, 2 units of 50 kW rated capacity wind turbine at 42m high and 90 units of 48V, 350Ah deep cycle batteries to meet the load demand. The capacity factors of solar, wind, and hybrid solar-wind power systems are 18%, 23%, and 21% respectively indicating high renewable energy resource potentials. The performances result also show slight complementarity between solar and wind power generation, thereby requiring battery backup to supplement the deficit

1.0 Introduction

Nigeria has been relying on fossil fuels to run its economy. These resources are finite and have adverse effects on the environment. It is therefore important to look for alternative sources that will meet the increasing energy demand while minimizing the negative environmental impacts Oyedepo (2012). Renewable energy resources such as solar and wind energies are promising in terms of power generation and are being considered as alternatives to fossil fuels due to their availability and topological advantages in local power generation and environmental friendliness (Hassan et al. 2023).

Renewable energy options are unpredictable in nature, and weather dependent and their variation may not match with the time distribution demand, therefore hybrid solar wind power systems with battery backup will attenuate their fluctuations significantly.
This study presents an evaluation of the performance of a designed and simulated hybrid solar-wind power system in the Heipang community (Kpang, Tapo, and Tatu) of Barkin-Ladi LGA of Plateau State based on the solar and wind energy resources potentials and the load demand of the community. This will provide information to government and non-governmental agencies for possible intervention in the community.

Many recent works have been carried out on the factors that influence the performance of solar and wind power systems. Dhass et al. (2020) studied the effect of temperature on internal parameters of various photovoltaic (PV) cell materials with results showing that temperature affects the performance of solar cells with GaAs and a-Si having major and minor deviations in performance. The study on the impacts of temperature and irradiance on polycrystalline silicon solar cell parameters using a metaheuristic technique was done by Fébba et al. (2018). The results of the study showed that the shunt and series resistance were more affected by the increasing temperature than by increasing irradiance, with a linear increase and decrease for series and shunt resistance, respectively. Similarly, the effect of light intensity and temperature on the performance parameters of monocrystalline and polycrystalline silicon solar devices was conducted (Amin and Al-Maghrabi, 2018). The experimental results showed that all electrical parameters of the solar cells such as maximum output power, open circuit voltage, short circuit current, and fill factor are affected by temperature variation and solar cell performance decreases with increase in temperature due to increase in carrier recombination rates. Guda and Aliyu (2015) developed a mathematical model for the photovoltaic array based on the equivalent electrical circuit of the solar cell. Results obtained competed favorably with those obtained through the use of the Manufacturers' datasheet and they were considered to be more accurate because they represented the actual field performance of the PV array. Ma et al. (2019) developed a mathematical model for solar photovoltaic modules. The developed model accurately produced characteristic curves for different PV modules and the validation of the model through comparison with measured curves achieved good agreement. Beniysa et al. (2019) used Newton Raphson's numerical method to develop a photovoltaic module model. The accuracy of the modeling was evaluated by comparing the modeled peak power to the reported experimental one provided by each photovoltaic module manufacturer which gave good agreement. Nacar et al. (2021) proposed a six-parameter single-diode model for photovoltaic modules to improve accuracy in estimating the electrical behavior of the modules using Particle swarm optimization and metaheuristic algorithms. The proposed model was tested and shown to predict the current voltage (I-V) curve with high accuracy. Site-specific wind turbine power curve or estimation of its power output was developed by Dongre and Pateriya, (2019). Different statistical methods based on empirical power curves were employed using techniques such as smoothing splines and polynomial regressions. The results showed

Corresponding author's e-mail address: mareni@unijos.edu.ng

that smoothing splines gave outstanding performance over all the other methods. Seo et al. (2019) developed a wind turbine power curve using the maximum likelihood estimation (MLE) method. The obtained logistic function closely follows the measured wind turbine powers. Teyabeen et al. (2018) carried out a comparative study of nine wind turbine power curves models based on manufacturers' power curve data. The accuracy of the models wasere evaluated using statistical criteria such as normalized root mean square error (NRMSE) and correlation coefficient. The power-coefficient-based model showed the most favorable efficiency. Dongre and Pateriya (2019) used statistical methods such as polynomial, splines and smoothing splines techniques to develop a site-specific power curve of a wind turbine to estimate its power output. The approach estimated the wind turbine power output accurately. Saha et al. (2023) carried out a simulation and modeling of a hybrid solar-wind power system in a MATLAB/Simulink environment using the Maximum Power Point Tracking (MPPT) method. The hybrid solar-wind systems provided reliable power and the MPPT enhanced energy outcome in varying conditions. Bangura et al. (2023) carried out a study on the modeling and simulation of a hybrid solar-wind energy system consisting of a photovoltaic cell and a wind turbine driven by a Permanent Magnet Synchronous Generator (PMSG). The proposed system achieved stable power flow under different weather conditions. Holmukhe et al. (2022) carried out a study on a hybrid solar-wind power system using MATLAB software to validate the system's reliability and economic feasibility. Results showed that the hybrid power system was more reliable and economically feasible than a solar or wind power system alone. Naggarapu et al. (2023) carried out battery modeling and performance analysis of time-varying load using MATLAB/Simulink tool to estimate the State of Charge (SOC) of autonomous vehicles. The proposed model achieved a root mean square error (RMSE) value of 0.1 and a widely acceptable SOC. Sawant et al. (2023) studied the role of battery energy storage in enhancing the reliability of wind-integrated power systems using the Sequential Monte Carlo Simulation (SMCS) approach. Results of the study showed that battery energy storage enhanced the reliability of wind-integrated power systems and the proposed operational strategy improved system reliability. Degla et al. (2022) carried out a study on how to improve the lithium-ion battery model for photovoltaic applications based on comparative analysis and experimental tests. Results showed that the Nernst model accurately predicted battery voltage with near-zero error. Shabani et al. (2021) carried out a study on the techno-economic impacts of battery performance models on the optimal design of a grid-connected PV system using a non-dominated sorting genetic algorithm. Results showed that battery models with accurate performance predictions give more efficient system optimization and a complex battery model gives a higher self-sufficiency ratio and lower life cycle cost. Ahammad and Shahidul (2014) used a sharing strategy to design a hybrid solar-wind power system for given load demand using the energy resources of Khulna and Chittagong in Bangladesh. Using different load scenarios, results show that a minimum unit cost of energy of $0.11/kWh was achieved in Khulna using average load and maximum solar radiation and wind speed.

The performance of a hybrid solar-wind power system is greatly influenced by the stochastic solar and wind energy resources of the location of operation. (Amirsaman et al. 2014). Many research works have been done on the design, simulation, and optimization of hybrid solar-wind power systems for different locations as highlighted in the literature reviewed, and to the best of the researchers' knowledge, little information appears to exist on the design of hybrid solar-wind power system using load sharing strategy and its performance in Heipang community. As highlighted in Rehman et al. (2020) resource potentials play a key role in the economics of the hybrid solar-wind power system and since the resources vary from location to location, it will be relevant to look at the performance

Corresponding author's e-mail address: mareni@unijos.edu.ng

of hybrid solar-wind power systems in Heipang community to provide relevant information to investors and policy makers.

2. Materials and Methods

2.1 Materials

The area at which this study was undertaken is in Barkin-Ladi L.G.A of Plateau State, Nigeria, and is located between longitudes 8° 50' E and 8° 59' E and between latitudes 9° 34' N and 9° 42' N (Land and Survey, 2018). The geomorphology of Heipang can be generally classified as plain land hence giving it the vantage position for the location of the airport.

The data used for the design and simulation of the hybrid solar-wind power system were 2018 hourly solar radiation, ambient temperature, and wind speed of Heipang community in Barkin-Ladi LGA measured at 10m height, obtained from the Nigerian Meteorological Agency office in Abuja. The estimated hourly load demand profile for a typical day in of Heipang community, not connected to the grid (Kpang, Tapo, and Tatu), was obtained from the field survey by means of a structured questionnaire and interview of the inhabitants of the community. MATLAB and Excel software were the tools used for analysis.

2.2 Design of Hybrid Solar-Wind Power System

2.2.1 Design considerations

The design of the hybrid solar wind power system entails the sizing of the power generating systems to meet the load demand of the community that are not connected to the grid. The two renewable energy resources considered in this design were solar and wind energies. The daily estimated load demand of the community under study was assumed to be constant throughout the year for simulation purpose.

2.2.2 Design concept

The design of the hybrid solar-wind power system for Heipang community is based on the percentage load sharing strategy approach (Ahmmad and Shahidul, 2014). The load was shared between solar and wind power generating systems.

2.2.3 Solar and wind energy potentials of site

The available solar energy potential per unit surface area of solar module in Heipang community was determined using a power output model for photovoltaic generator developed by Hybrid Optimization of Multiple Electric Renewables (HOMER, 2016) using equations 1 to 3.

$$P_{PV} = N_{PV} \times \frac{Y_{pv}}{1000} f_{pv} \left(\frac{G_T}{G_{T,STC}}\right)\left[1 + \alpha_p (T_c - T_{c,STC})\right] kW \quad (1)$$

$$\eta_{mp,STC} = \frac{Y_{pv}}{A_{pv} * G_{T,STC}} \quad (2)$$

$$T_c = \frac{T_a + (T_{c,NOCT} - T_{a,NOCT})\left(\frac{G_T}{G_{T,NOCT}}\right)\left[1 - \frac{\eta_{mp,STC}(1 - \alpha_p \times T_{c,STC})}{\tau\alpha}\right]}{1 + (T_{c,NOCT} - T_{a,NOCT})\left(\frac{G_T}{G_{T,NOCT}}\right)\left(\frac{\alpha_p \times \eta_{mp,STC}}{\tau\alpha}\right)} \quad (3)$$

where, P_{PV} is power generated by solar system at time (kW), N_{PV} is number of photovoltaic modules, Y_{pv} is rated capacity of the solar module, f_{pv} is photovoltaic derating factor, G_T is solar radiation normal to inclined plane (W/m^2), $G_{T,NOCT}$ is solar radiation at nominal operating solar cell (W/m^2),

Corresponding author's e-mail address: mareni@unijos.edu.ng

$G_{T,STC}$ is incident solar radiation at standard test condition (W/m^2), α_p is temperature coefficient of power, T_c is solar cell temperature (°C), $\eta_{mp,STC}$ is maximum power point efficiency under standard test (%), A_{pv} is surface area of the solar module (m^2), T_a is ambient temperature of location of study (°C), $T_{c,NOCT}$ is nominal operating solar cell temperature (°C), $T_{a,NOCT}$ is ambient temperature at nominal operating temperature (°C), $\tau\alpha$ is solar transmittance-absorptance factor of solar module cover.

The available wind energy potential per unit surface area of wind turbine system in Heipang community was determined using equations 4 and 5.

$$v = v_0 \left(\frac{H_{WT}}{H_0}\right)^{\alpha_1} \tag{4}$$

where, v is wind speed at hub height (m/s), v_o is wind turbine cut-out wind speed (m/s), H_{WT} is wind turbine hub height (m), H_0 is reference height for measuring wind speed (m), α_1 is power law exponent.

The best fit power output model for the wind turbine selected (FD21-50) as determined by means of least square method in the course of this research (Maren et al., 2022) is given as:

$$P_{wt} = N_{WT}\begin{cases} P_R \dfrac{v^{2.5} - v_C^{2.5}}{v_R^{2.5} - v_C^{2.5}} & v_C \le v < v_R \\ P_R & v_R \le v \le v_F \\ 0 & v < v_C; v > v_F \end{cases} \tag{5}$$

2.2.4 Load sharing strategy of the solar-wind power system

According to equations 1 and 5, the power generated by the photovoltaic module per unit area is P_{pva} and power generated by wind turbine per unit area is P_{wta} respectively. Thus, the load shared by the solar power generation system and the wind power generation system of the proposed hybrid system are given by the equations 6 and 7 respectively.

Load shared to the photovoltaic module of the hybrid system was determined using equation 6 ~~is~~ (Ahammad and Shahidul, 2014):

$$P_{sh} = \frac{P_{pva}}{P_{pva}+P_{wta}} \times P \tag{6}$$

where: P is the total load of appliances of Heipang community not connected to the grid (Kpang, Tapo and Tatu) in kW~~.~~, P_{pva} is power generated by photovoltaic per unit area (kW/m^2), P_{wta} is power generated by wind turbine per unit area (W/m^2).

Load shared to the wind turbine of the hybrid system is (Ahammad and Shahidul, 2014):

$$P_{wh} = \frac{P_{wta}}{P_{pva}+P_{wta}} \times P \tag{7}$$

where: P is the total load of appliances of Heipang community not connected to the grid (Kpang, Tapo and Tatu) in kW-, P_{pva} is power generated by photovoltaic per unit area (kW/m^2), P_{wta} is power generated by wind turbine per unit area (W/m^2).

2.2.5 Sizing and selection of photovoltaic module

The power from the photovoltaic module should be able to meet the percentage of load allotted to it based on the solar potential in the site. If the load allotted to the photovoltaic system is P_{sh}, then the number of photovoltaic modules required to serve the load is:

$$N_{PV} = \frac{P_{sh}}{P_{rs}} \quad (8)$$

where: P_{sh} is solar power system load share (kW), P_{rs} is power rating of the selected photovoltaic module (kW).

The photovoltaic module randomly selected for this research work was the WON300 mono-crystalline model (WUXI Technology, 2019). The solar panel was selected because of its relatively higher efficiency when it was tested and compared with other monocrystalline solar panels available in market (NOA Testing Inspection Technology. 2018).

2.2.6 Sizing and selection of wind turbine

From equation 7 the load allotted to the wind turbine system is P_{wh}, thus, the number of wind turbines required to serve the load is:

$$N_{WT} = \frac{P_{wh}}{P_{rw}} \quad (9)$$

where: P_{sh} is solar power system load share (kW), P_{rw} is power rating of the selected Wind turbine (kW)

The wind turbines selected for the design was FD21-50 model (Ghrepower, 2020). It was selected because of its high-power output performances in Heipang wind speed regime as analyzed in the course of this research.

Battery was used to store excess energy or supply when there was energy deficit. Battery life was affected by its depth of discharge. Deep cycle batteries discharge 50-80% of their capacity (Izdin.Hlal et al., 2019).

The battery capacity required to supply the full load demand was determined using equation 10 (Tharani and Dahiya, 2018).

$$C_{wh} = \frac{E_L \times S_D}{\eta_{bat}} \quad (10)$$

where: E_L is electrical load (kW), SD is battery day of autonomy (day), η_{bat} is efficiency of battery (%)

The number of batteries in parallel was computed using equation 11:

$$N_{bp} = \frac{C_{wh}}{C_{ah} \times V_B} \quad (11)$$

where: C_{wh} is capacity of battery (Wh), C_{ah} is ampere-hour rating of the selected battery (Ah), V_B is nominal voltage of the selected battery (V).

The number of batteries in series was obtained by equation 12:

$$N_{bs} = \frac{V_{system}}{V_B} \quad (12)$$

where: V_{system} is hybrid solar-wind power system voltage (V), V_B is nominal voltage of the selected battery (V).

The storage battery selected for the design was Hoppecke 24 OPzVsolar.power 3500 - 48V.This type of battery can be effectively used in sectors applicable with high charging and discharging operation such as in solar and other off-grid applications (Europe Solarstore, 2023).

2.2.7 Sizing and selection of inverter

The DC/AC converter, also known as inverter was used to convert DC signal from the battery to AC signal to supply to load.

Inverter power $P_{INV}(t)$ was determined using the corresponding load power requirements, as follows (Ghenai et al., 2020):

$$P_{INV}(t) = \frac{P_{load}(t)}{\eta_{INV}} \quad (13)$$

where: $P_{load}(t)$ is power consumed by the load at hour t (kW), η_{INV} is inverter efficiency (%) SKU-ATO-OGI-200kW inverter was selected for this study (Inverter.com, 2021).

2.3 Simulation of Hybrid Solar-Wind Power System

MATLAB programme codes were written to simulate the designed system to determine the performance indices such as: hourly power generated by solar and wind energy conversion systems, Loss of power supply probability, battery state of charge and the capacity factors of the renewable energy system, using equations 1 to 29.

Equations 14 to 20 were used to convert solar radiation normal to the horizontal to that normal to the inclined plane corresponding to the plane of the photovoltaic (Duffie et al., 2020).

(i) Angle of declination δ given as:

$$\delta = 23.45 \times Sin\left[\frac{360}{365}(284 + n_d)\right] \quad (14)$$

where: n_d is number of the days in a year

(ii) The hourly extraterrestrial solar radiation is the radiation beyond the atmosphere and is computed from the expression:

$$G_E = G_{sc}\left(1 + 0.033cos\left(\frac{360 \times n_d}{365}\right)\right)(cos\phi cos\delta sin\omega_{1-24} + sin\phi sin\delta) \quad (15)$$

where: G_{sc} is solar constant 1367 (W/m^2), n_d is number of the days in a year, δ is angle of declination (degree), ϕ is latitude of the location (degree), ω is hour angle (degree).

(iii) The clearness index relates the measured global radiation in the atmosphere to the extraterrestrial radiation and is computed from the expression:

$$K_T = \frac{G_m}{G_E} \quad (16)$$

where: G_m is measured daily global solar radiation on horizontal surface (W/m^2), G_E is hourly extraterrestrial solar radiation (W/m^2).

(iv) The diffuse component of the total solar radiation is computed from:

$$G_d = G_m \times \begin{cases} 1.0 - 0.249K_T & for\ K_T < 0.35 \\ 1.557 - 1.84K_T & for\ 0.35 < K_T < 0.75 \\ 0.177 & for\ K_T > 0.75 \end{cases} \quad (17)$$

where: G_m is measured daily global solar radiation on horizontal surface (W/m^2), K_T is clearness index

(v) The beam radiation on a horizontal plane can be computed from the relation:

$$G_b = G_m - G_d \quad (18)$$

G_m is measured daily global solar radiation on horizontal surface (W/m^2), G_d is diffuse solar radiation (W/m^2)

(vi) The ratio of flux of beam radiation on an inclined surface to that on the horizontal surface R_b is computed from:

$$R_b = \frac{cos(\phi-\beta')cos\delta cos\omega + sin(\phi-\beta')sin\delta}{cos\phi cos\delta cos\omega + sin\phi sin\delta} \quad (19)$$

where: G_{sc} is solar constant 1367 (W/m^2), n_d is number of the days in a year, δ is angle of declination (degree), ϕ is latitude of the location (degree), ω is hour angle (degree), $\acute{\beta}$ is inclined angle of solar panel to the horizontal plane (degree)

(vii) The solar radiation normal to inclined angle equal to the solar panel inclination to horizontal plane or latitude of the location is estimated from:

$$G_T = G_b R_b + G_d\left(\frac{1+cos\beta'}{2}\right) + G_m\rho_g\left(\frac{1-cos\beta'}{2}\right) \quad (20)$$

where: G_b is beam radiation on a horizontal plane (W/m^2), G_d is diffuse solar radiation (W/m^2), G_m is measured daily global solar radiation on horizontal surface (W/m^2), R_b is ratio of beam radiation on an inclined surface to that on the horizontal surface, ρ_g is diffuse reflectance of the surroundings, $\acute{\beta}$ is inclined angle of solar panel to the horizontal plane (degree).

2.3.1 Wind power output model

The wind power output model used for the simulation of the designed system was computed using equations 4 and 5. The MATLAB codes uses equation 4 to convert the wind speed $v_o$measured at 10m height at the weather station to the height of the wind turbine hub, which was used as input in equations 5.

2.3.2 Solar power output model

Model-1: HOMER model for solar power output developed by Hybrid Optimization of Multiple Electric Renewables (HOMER) given in equation 1 to 3 was used in the simulation.

Model-2: Using the solar radiation available on the tilted surface, the ambient temperature and the manufacturers data of the PV modules as model inputs, the power output of the PV generator, P_{PV} was calculated using equation 21 and 22 which was also used in the simulation (Zhou, 2007).

$$P_{PV} = \frac{N_{PV}}{1000} \times \frac{v_{oc} - ln(v_{oc}+0.72)}{1+v_{oc}} \times \left[1 - \frac{R_s}{V_{oc}/I_{sc}}\right] \times \frac{V_{oco}}{1+\beta ln\left(\frac{G_o}{G_T}\right)} \times \left(\frac{T_o}{T_c}\right)^{\gamma} \times I_{sco} \left(\frac{G_T}{G_o}\right)^{\alpha} kW \quad (21)$$

$$T_c = T_a + \frac{G_T (T_{c,NOCT} - T_{a,NOCT})}{G_{T,NOCT}} \quad (22)$$

where: N_{PV} is number of photovoltaic modules, v_{oc} is normalized value of the open circuit voltage to the thermal voltage (V), R_s is photovoltaic module series resistance (Ω), V_{oc} is open-circuit voltage of the photovoltaic module under standard test condition (V), I_{sc} is short-circuit current of the photovoltaic module under standard test condition (A), I_{sco} is short-circuit current of the photovoltaic module under the standard solar radiation, G_o (A), V_{oco} is open-circuit voltage of the photovoltaic module under the standard solar radiation G_o (V), β is photovoltaic module technology specific-related dimensionless coefficient, G_o is standard solar radiation 1000W/m^2, G_T is solar radiation normal to inclined plane (W/m^2), T_o is temperature of the photovoltaic module at standard condition 25°C (°C), T_c is solar cell temperature (°C), γ is exponent considering all the non-linear temperature-voltage effect, α is factor responsible for all the non-linear effects that the photovoltaic depends on, T_a is ambient temperature of location of study (°C), $T_{c,NOCT}$ is nominal operating solar cell temperature (°C), $T_{a,NOCT}$ is ambient temperature at nominal operating temperature (°C), $G_{T,NOCT}$ is solar radiation at nominal operating solar cell (W/m^2), T_a is ambient temperature of location of study (°C)

However, the five parameters $(\alpha, \beta, \gamma \text{ and } R_s)$ in the model equation 21 were determined from the solar panel parameters measured by solar or flash simulator at the NOA Testing and Inspection Technology Ltd, Building 26, No. 2777, East Jinxiu Road, Shanghai, China (NOA Testing Inspection Technology. 2018).

2.3.3 Battery capacity model

The initial storage capacity of the battery is computed as (Tharani and Dahiya, 2018):

$$C_{wh} = C_{bat}(t-1) = \frac{E_L \times S_D}{\eta_{bat}(1-DOD)} \quad (23)$$

where: $C_{bat}(t-1)$ is battery bank capacity at hour (t-1) (Wh), E_L is electrical load (kW), SD is battery day of autonomy (day), η_{bat} is efficiency of battery (%), DOD is depth of discharge (%).

In case when the battery capacity reaches a maximum value, C_{batmax}, the control system stops charging process. During the charging process, when the total output of PV module and wind generators is greater than the load demand, the available battery bank capacity at hour t can be determined as (Izdin.Hlal et al., 2019):

$$C_{bat}(t) = C_{bat}(t-1).(1-\sigma) + \left(P_{PV}(t) + P_{WT}(t) - \frac{P_{load}(t)}{\eta_{inv}}\right).\eta_{batC} \quad (24)$$

On the other hand, the battery discharges when the load demand is greater than the available energy generated. Thus, the capacity of the battery bank at any time t in hour can be expressed as (Izdin.Hlal et al., 2019):

$$C_{bat}(t) = C_{bat}(t-1).(1-s) - \left(\frac{P_{load}(t)}{?_{inv}} - (P_{PV}(t) + P_{WT}(t))\right)\eta_{batD}?_{batD} \quad (25)$$

where:

$C_{bat}(t-1)$ is battery bank capacity at hour (t-1) (Wh), σ is self-discharge rate of the battery bank, $P_{PV}(t)$ is power generated by solar system at time t (kW), $P_{WT}(t)$ is power generated by wind turbine at time t (kW), $P_{load}(t)$ is power consumed by the load at hour t (kW), η_{inv} is inverter efficiency (%), η_{batC} is battery efficiency during charging process (%), η_{batD} is battery efficiency during discharging process (%).

Charging constraint

$$C_{bat}(t) \leq C_{bat\ max}$$

Discharging constraint

$$C_{bat}(t) \geq C_{bat\ min}$$

$$C_{bat\,min} = DOD \times C_{bat\,max} \quad (26)$$

where:

$C_{bat\,min}$ is minimum capacity of battery (Wh), DOD is depth of discharge (%) =50%, C_{batmax}. is maximum capacity of battery $= 1{,}512kWh$

2.3.4 Energy management strategy of hybrid solar wind power system

The role of control strategy management in hybrid solar-wind power system is very important in system operation. This is because a proper control system increases system efficiency, the power availability, the amount of power generated and the life span of the battery system while decreasing the number of deficit hours and the amount of dumped load of the system (Sigarchian et al., 2014).

The proposed energy management of the hybrid solar-wind power system is summarized as follows:

Case 1

If $P_{gen} > P_{load}$ and $SOC(t-1) < SOC_{max}$ then satisfy the load and charge the battery with the surplus power.

Case 2

If $P_{gen} > P_{load}$ and $SOC(t-1) \geq SOC_{max}$ then stop charging the battery, satisfy the load. Excess power is dumped.

Case 3

If $P_{gen} < P_{load}$and $DOD(t-1) > DOD_{max}$ then satisfy the load by discharging the battery to cover the deficit in load power

Corresponding author's e-mail address: mareni@unijos.edu.ng

Case 4

If $P_{gen} < P_{load}$ and $DOD(t-1) \geq DOD_{max}$ then stop battery discharging. There is power deficit.

where: P_{gen}, is the total power generated by solar and wind power systems, P_{load}, is the load demand of Heipang community, $SOC(t-1)$, is the battery state of charge in time $(t-1)$, SOC_{max}, is the maximum state of charge of battery, $DOD(t-1)$, is the battery depth of discharge at time $(t-1)$, DOD_{max}, is the maximum depth of discharge of battery.

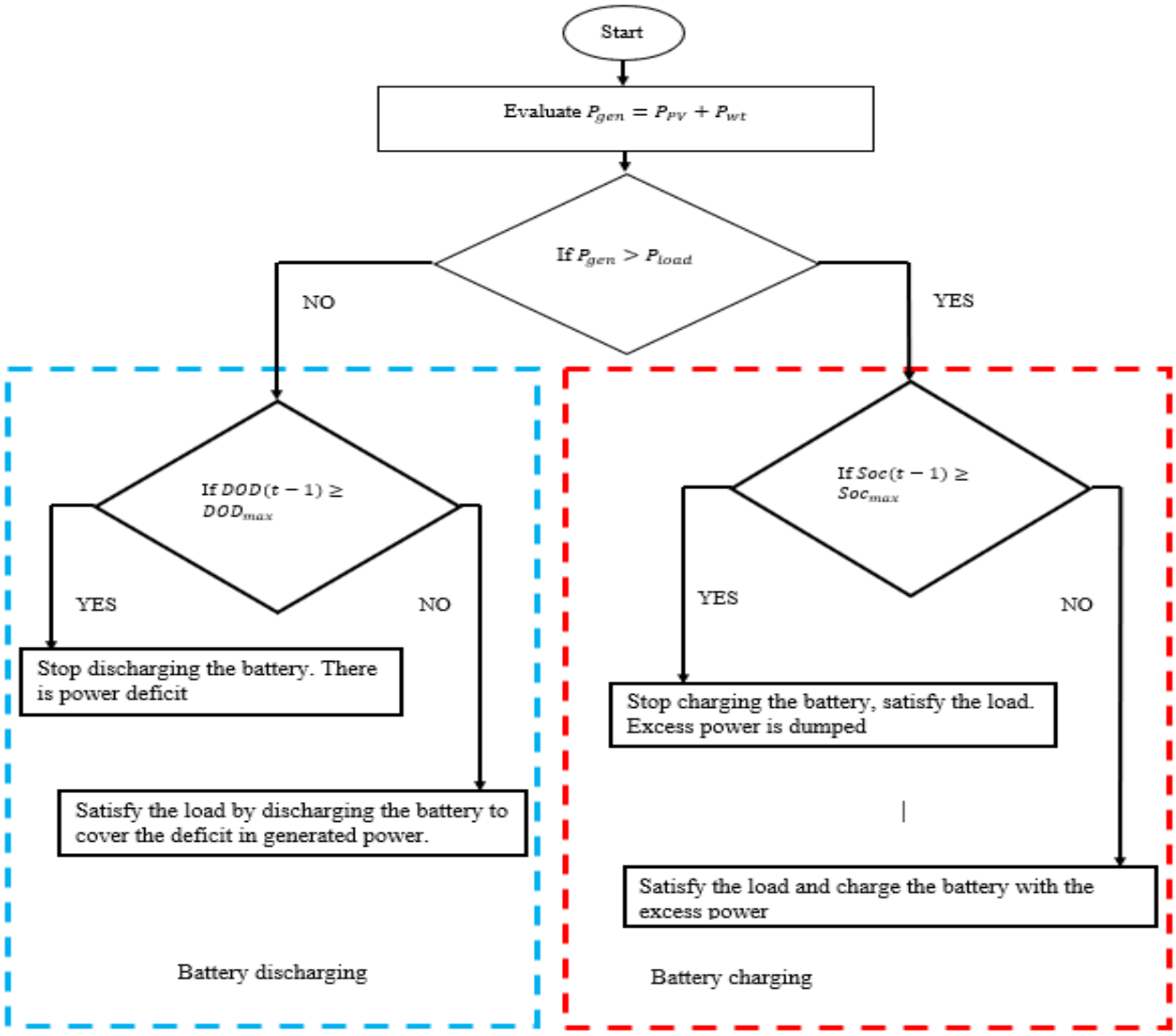

Figure 1: Energy management strategy flow chart of hybrid solar-wind power system

2.3.5 Hybrid solar wind power system total energy generation

The total annual energy generation by the hybrid solar wind power system is computed as follows:

$$\sum_{t=1}^{T} P_h(t) = \sum_{t=1}^{T}\left(P_{pv}(t) + P_{WT}(t)\right)\Delta t \quad (27)$$

where: $P_h(t)$ is hybrid solar-wind power generated at time (t) (kW), $P_{pv}(t)$ is power generated by solar system at time t (kW), $P_{wt}(t)$ is power generated by wind turbine at time t (kW), Δt is time step used for simulation (hr).

2.3.6 Capacity factor of hybrid solar-wind power system

The ratio of the actual power generated to the power it would have generated if operating at its rated capacity in one year is the capacity factor of a power system. The capacity factor of the hybrid (solar-wind) power system was determined from (Center for Sustainable Systems, 2023):

$$CF_{Hybrid} = \left(\frac{\sum_{1}^{T}\left((P_{PV}(t)+P_{WT}(t)).\Delta t\right)\eta_{inv}}{P_{Hybrid}\times T}\right) \quad (28)$$

where: $P_h(t)$ is hybrid solar-wind power generated at time (t) (kW), $P_{PV}(t)$ is power generated by solar system at time t (kW), $P_{WT}(t)$ is power generated by wind turbine at time t (kW), P_{Hybrid} is hybrid solar-wind power generated (kW), T is operation time (8760) of hybrid solar wind power system (hr), η_{inv} is inverter efficiency (%),

2.3.7 Total available energy generation for load demand

The total energy, $P_{total}(t)$ generated by the wind turbine and PV generator at hour t to meet a demand at hour t is calculated as follows: i.e., energy generated by solar and wind plus the energy stored in battery.

$$P_{total}(t) = \left((P_{PV}(t) + P_{WT}(t)).\Delta t + C_{bat}(t-1) - C_{batmin}\right)\eta_{inv} \quad (29)$$

$C_{bat}(t-1)$ is battery bank capacity at hour (t-1) (Wh), $P_{PV}(t)$ is power generated by solar system at time t (kW), $P_{WT}(t)$ is power generated by wind turbine at time t (kW), Δt is time step used for simulation (hr), $C_{bat\,min}$ is minimum capacity of battery (Wh), η_{inv} is inverter efficiency (%).

3. Results and Discussion

3.1 Designed Hybrid Solar-Wind Power System

Based on the load sharing strategy design approach, 283 units of 300W capacity solar panels, 2units of 50 kW rated capacity wind turbine at 42m high and 90 units of 48V, 350Ah deep cycle battery will be required to meet the estimated load demand of 158.32 kW and a daily energy demand of 710.59 kWh/day, with two days autonomy (Figure 2).

Corresponding author's e-mail address: mareni@unijos.edu.ng

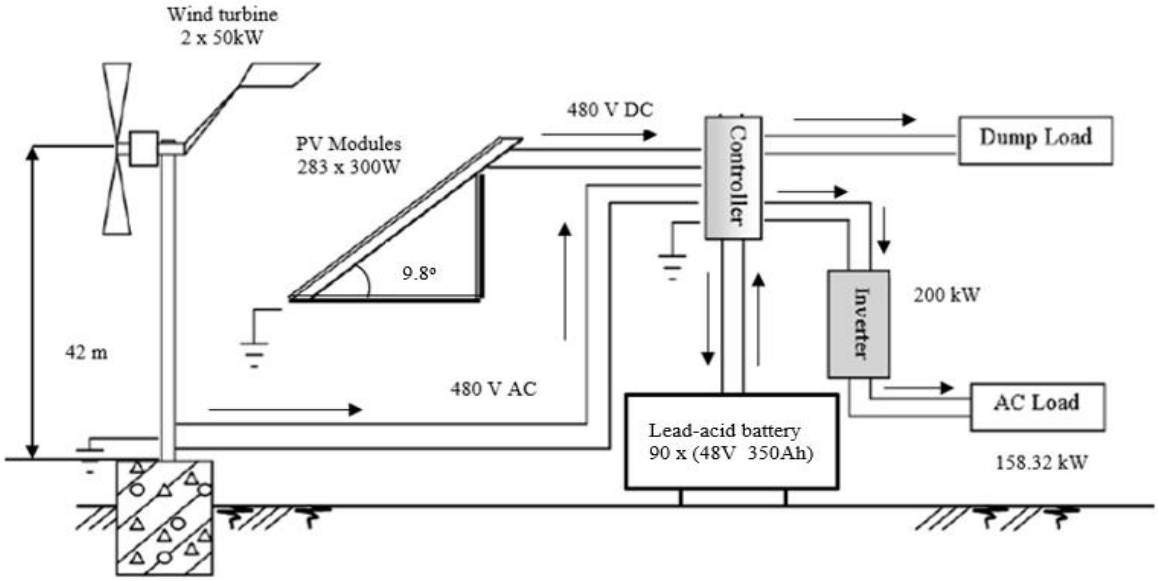

Figure 2: Diagram of the designed hybrid solar-wind power system

3.2 Simulation of Hybrid Solar-Wind Power System

3.2.1 Solar power output

Figure 3 (a, b, c and d) shows the plot of the power output of photovoltaic system against time for different hours of the day and different days of the year under consideration. There is a correlation between the simulation results of the solar power output of the photovoltaic system using solar power model 1 developed by (HOMER, 2016) as given by equation 1 and solar model 2 developed by (Zhou, 2007) as given by equation 21. The results show a high level of correlation value of 0.9998, between solar power models 1 and 2 and can thus be used interchangeably. The solar power generated corresponds to the intensity of the incident solar radiation, which increases from morning hours (7: 00 am) when the solar intensity is low and peaks up around afternoon hours, when there is no cloud and declines as the sun sets in the evening. Similarly, the models correlate throughout the seasons of the year depending on the diurnal and seasonal variation of the solar radiation in the location of study. The plots also show a close superimposition of the solar power models thereby substantiating the high correlation between the models.

Corresponding author's e-mail address: mareni@unijos.edu.ng

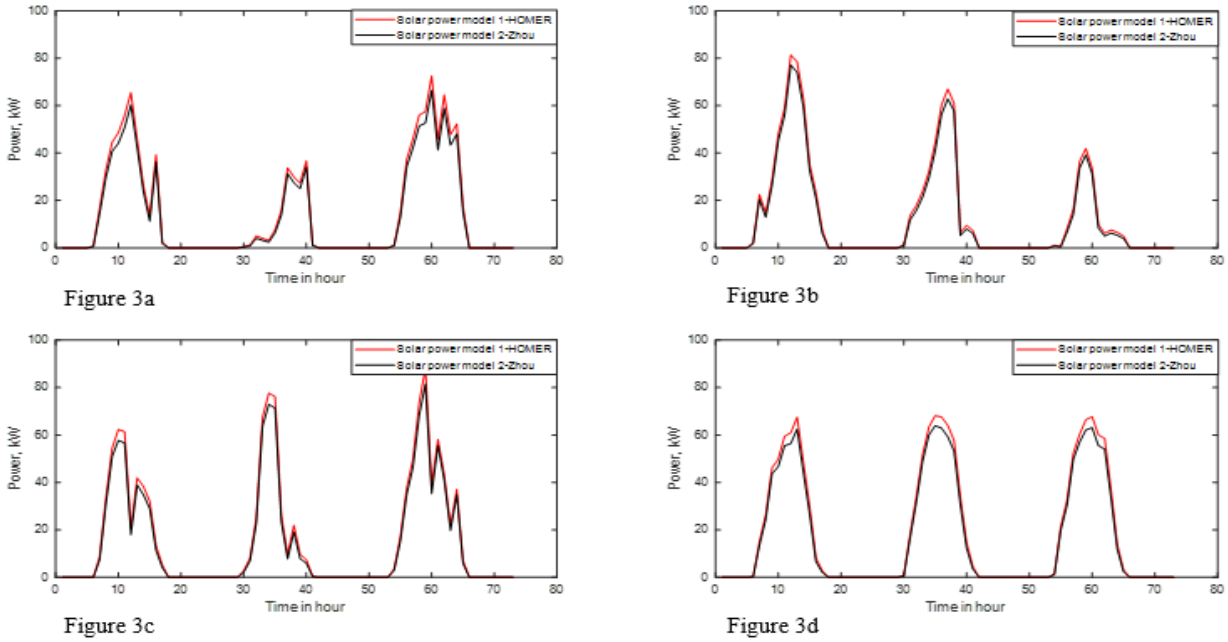

Figure 3: Plots of Power Output pf Photovoltaic System against time

3.2.2 Solar and wind power output

Figure 4 (a, b, c and d) presents the plots of the solar and wind power generated against time for different months of the year under review, with solar and wind energy penetration of 48%, 52% in March, 40%, 60% in June, 30%, 70% in September and 42% and 58% in December respectively. As shown in the figures, wind power yield is relatively more stochastic than solar and cannot provide stable power supply if used alone. Based on the simulation of the hybrid solar wind power system, annual performance assessment of the system shows that the solar power system has a capacity factor of 18%, higher than that in Cirata, Indonesia which 15% (Febrian et al., 2023). Wind power system has a capacity factor of 23% which is over 20%, lower than that in USA which ranges from 21% to 52% and averages 35% (Center for Sustainable Systems, 2023) and the hybrid solar wind power system having capacity factor of 21%. This is an indicator of high solar and wind energy potentials in Heipang community. The plot also shows some level of complementarity between the solar and wind energy generation as wind energy is generated in the night hours when there is no sunshine. The complementarity is measured by the coefficient of correlation which gives a value 0.24. If the coefficient of correlation is 1, the two renewable sources vary in the same way and when it is -1, they vary in opposite way which shows good complementarity. In figure 4b, there is complementarity for hours between 6:00 PM of the first day to 8:00 AM the next day and between 6:00 PM of the second day to 8:00 AM the third day. Similarly, in figure 4c, the solar and the energy show good complementarity between the 15 to 30 hours. However, in the late hours of the third day there is power deficit to meet the load and that is where the battery backup role comes to play.

Corresponding author's e-mail address: mareni@unijos.edu.ng

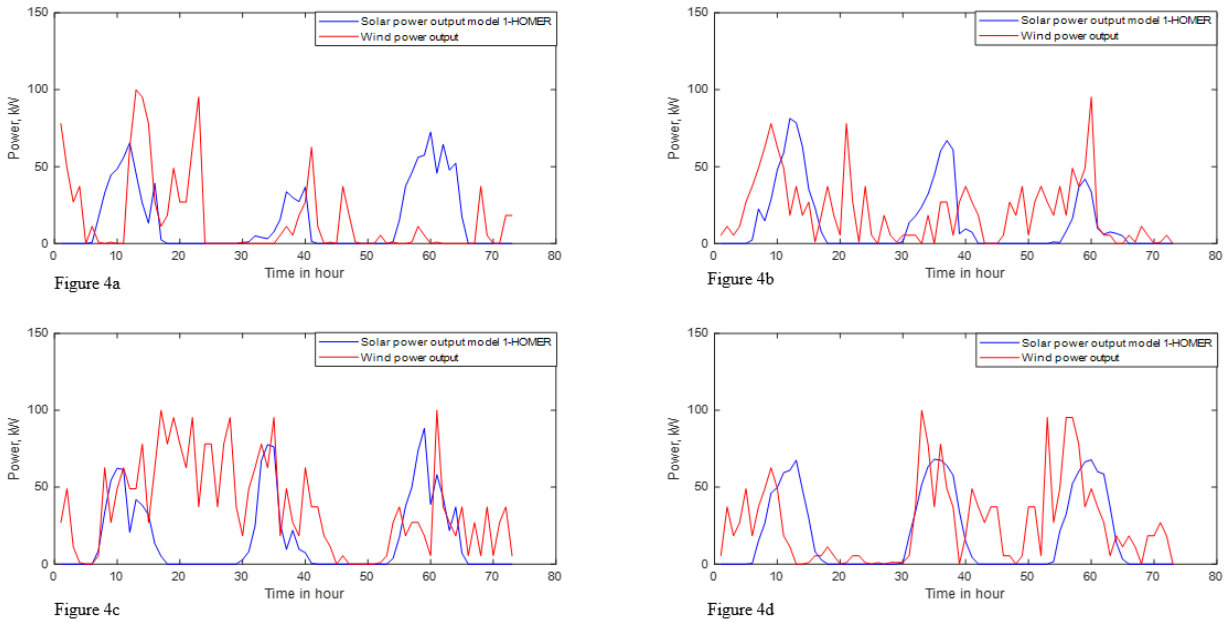

Figure 4: Plots of Solar and Wind Power Generated and Load Demand against time

3.2.3 Hybrid solar-wind power generated, load demand and state of charge of battery of system

Figure 5 (a, b, c and d) shows a three-day plot of hybrid solar-wind power, battery stored energy and load demand over hours of the days for different months of the year under review. The designed system is based on 2 days autonomy, meaning the battery can supply power for two consecutive days when there is no power generation by either solar, wind or both power systems which is the minimum requirement for solar wind power system design (Adeoye et al., 2022), (Broomfield Designers, 2017). Based on the simulation plot the energy in the battery meets the load demand of the Haipang community. As shown in the figures, the battery complements the power deficit of the hybrid solar-wind power system, thereby meeting the load demand of Heipang community. In extreme cases where the battery fails to meet the load demand, there will be power deficit. This problem can be solved

Corresponding author's e-mail address: mareni@unijos.edu.ng

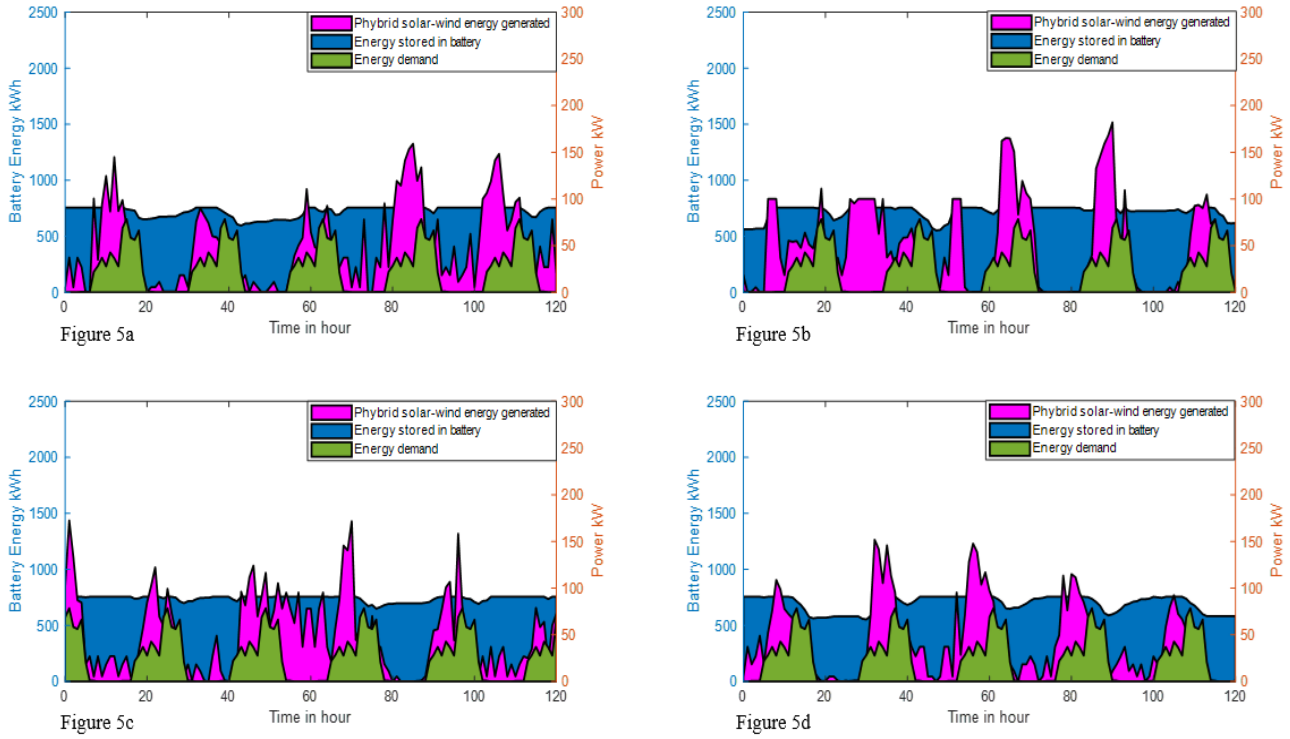

Figure 5: Plot of hybrid solar-wind power generated, battery energy and load demand against time

Figure 6 (a, b, c, d and e) shows the annual simulation plot of solar-wind power, and load demand, battery SOC in kWh, deficit load, dump load and battery SOC in % against time. Based on the simulation results shown in figures 6a 6b, 6c, 6d and 6e, the hybrid system has an annual load deficit of -2676.81kW and an excess load of 117, 676.89kW as generated by the solar-wind power system as obtained. The battery state of charge depends on the energy generated and the load demand at any time. In figure 6b the plot trend shows the SOC of the battery is high enough to meet the load demand except between 1000 and 2000 hours point and between 4000 to 7000 hours where the SOC drops to minimum SOC (SOCmin) which results to power deficit as shown in figure 6c. Figure 6d shows dump load plot with the excess power generated corresponding with when there is high energy generation by the hybrid solar-wind power system. The question that comes to mind is why the deficit when there is excess power generated? This is because renewable energy generation is stochastic in nature so the energy generated may not occur corresponding to the load demand. Thus, sometimes there will be moments of excess generation when the load is at its lowest or deficit when the load demand is at its peak when there is no power generation by the hybrid system. Backup battery reduces the dump load as excess power is stored in the battery after meeting the load demand. One of the ways to reduce the excess or deficit power generation is by optimal design of the hybrid solar-wind power system.

Corresponding author's e-mail address: mareni@unijos.edu.ng

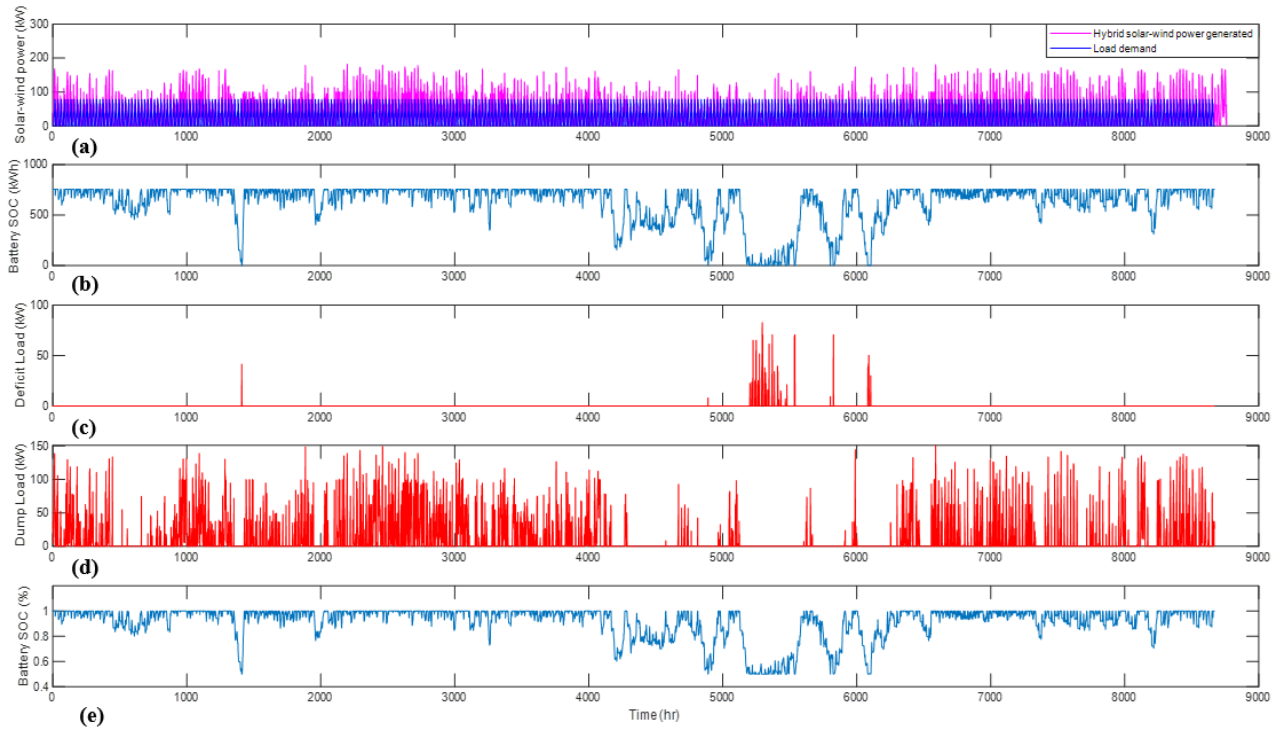

Figure 6: Plot of annual simulation of (a) solar-wind power and load demand (b) Battery SOC in kWh (c) Deficit load (d) Dump load and (e) Battery SOC in % against time.

4. Conclusion

A hybrid solar-wind power system was designed to meet the load demand of Haipang community not connected to the grid. For a load demand of 158.32 kW and a daily energy demand of 710.59 kWh/day, with two-day autonomy, the system capacity to meet the load demand comprise of 283 units of 300W solar panels, 2 units of 50 kW rated capacity wind turbine at 42m high and 90 units of 48V, 350Ah deep cycle batteries. Simulation result of the system shows that the designed system meets the load demand of the community with an annual excess power generation of 128,394.02kW and a deficit of 2676.81kW. The capacity factor of the hybrid solar-wind power system is 21% which compete favorably with solar generation in other countries such as Indonesia which is 15%. This shows that it is feasible to design a hybrid solar-wind power system to meet the load of Heaipang community. There is slight complementarity between solar and wind power generation, the battery backup system enhances the efficient performance of the hybrid solar-wind power system and reduce energy deficit and dump load. Optimal design of the hybrid solar-wind power system will further reduce the excess and deficit power of the system.

Corresponding author's e-mail address: mareni@unijos.edu.ng

References

Adeoye, O., Cofie, P. and Abood, S. 2022. PV Solar Battery Sizing Autonomy for Residential Applications Photovoltaic Solar Battery Sizing Autonomy for Residential Applications. American Society for Engineering Education, 5: 1-8.

Ahammad, M. and Shahidul, IK. 2014. Design Strategy for Aan Off-Grid Solar-Wind Hybrid Power System. (Master's thesis, Bangladesh University of Engineering and Technology, Dhaka, Bangladesh).

Amin, AAE., and Al-Maghrabi, MA. 2018. The Analysis of Temperature Effect for mc-Si Photovoltaic Cells Performance. Silicon, *10*: 1551–1555.

Amirsaman, A., Mahmoud, G., Mehdi, E. and Mohammed, SF. 2014. Stochastic Performance Assessment and Sizing for a Hybrid Power System of Solar/Wind/Energy Storage. IEEE Transactions on Sustainable Energy, 5(2): 363-371.

Bangura, AA., Errouha, M., Hihi, H. and Chalh, Z. 2023. Modelling and Simulation of the Hybrid System PV-Wind. Statistics, Optimization and Information Computing, 11(1): 143–153.

Beniysa, M., El Idrissi, AJ., Bouajaj, A. and Britel, MR. 2019. An Iterative Approach for Modeling a Photovoltaic Module using the Complete Single-Diode Model. 2019 International Conference on Intelligent Systems and Advanced Computing Sciences (ISACS), held in Taza, Morocco, 04-06 May 2023, pp. 1-5.

Broomfield Designers. 2017. Sun Xtender Solar Batteries - Photovoltaic Battery. https://www.sunxtender.com/battery_sizing.php accessed on 20 June, 2023.

Center for Sustainable Systems. 2023. Wind Energy Factsheet: Wind Resource and Potential. University of Michigan, Ann Arbor, USA. https://css.umich.edu/publications/factsheets/energy/wind-energy-factsheet accessed on 10 August, 2023.

Degla, A., Chikh, M., Mahrane, A. and Hadj Arab, A. 2022. Improved lithium-ion battery model for photovoltaic applications based on comparative analysis and experimental tests. International Journal of Energy Research, *48*(6): 10965–10988.

Dhass, A., Prakash, Y. and Ramya, K. 2020. Effect of temperature on internal parameters of solar cell. Materials Today: Proceedings, 30: 732–735.

Dongre, B. and Pateriya, RK. 2019. Statistical power curve modeling to estimate wind turbine power output. Wind Engineering, *43*(3): 213–224.

Duffie, JA., Beckman, WA. and Blair, N. 2020. Solar Engineering of Thermal Processes, Photovoltaics and Wind, Fifth Edition. John Wiley and Sons Inc., New Jersey.

Europe Solarstore. 2023. Hoppecke 5 OPzS solar. Power 350 - 48V. https://www.europe-solarstore.com/hoppecke-5-opzs-solar-power-350-48v.html accessed on 12 September, 2023.

Fébba, DM., Rubinger, RM., Oliveira, AF. and Bortoni, EC. 2018. Impacts of temperature and irradiance on polycrystalline silicon solar cells parameters. Solar Energy, 174: 628–639.

Febrian, HG., Supriyanto, A. and Purwanto, H. 2023. Calculating the energy capacity and capacity factor of floating photovoltaic (FPV) power plant in the cirata reservoir using different types of solar panels. Journal of Physics: Conference Series, 24(1): 1-22.

Ghenai, C., Rasheed, MA., Alshamsi, MJ., Alkamali, MA., Ahmad, FF. and Inayat, A. 2020. Design of Hybrid Solar Photovoltaics/Shrouded Wind Turbine Power System for Thermal Pyrolysis of Plastic Waste. Case Studies in Thermal Engineering, 22: 100773.

Corresponding author's e-mail address: mareni@unijos.edu.ng

Ghrepower. 2020. D21-60/FD21-100 Best Model for Commercial Electricity Generation. http://en.ghrepower.com/fd21-series/ accessed on 17 September, 2023.

Guda, HA. and Aliyu, UO. 2015. Experimental Determination of Photovoltaic Array Model Parameter. International Journal of Engineering and Technology, 5(2): 95–104.

Holmukhe, RM., Gandhar, A., Hans, D. and Paithankar, PV. 2022. A simulation study of solar wind hybrid power system. Journal of Information and Optimization Sciences, 43(3): 601–606.

HOMER. 2016. HOMER Pro Version 3.7 User Manual. https://homerenergy.com/products/pro/docs/index.html accessed on 13 June, 2023.

Inverter.com. 2021. 200kW Pure Sine Wave Off Grid Solar Inverter. https://www.inverter.com/200kw-pure-sine-wave-off-grid-solar-inverter accessed on 19 October, 2023.

Izdin-Hlal, M., Ramachandaramurthy, VK., Hafiz Nagi, HF. and Abdullah, R. 2019. Optimal Techno-Economic Design of Standalone Hybrid Renewable Energy System Using Genetic Algorithm. IOP Conference Series: Earth and Environmental Science, 268(1): 15-25.

Land and Survey. 2018. A Map of Heipang Community, Barkin-Ladi L. G. A, Plateau State, Nigeria.

Ma, T., Wenbo, G., Lu, S. and Meng, L. 2019. An improved and comprehensive mathematical model for solar photovoltaic modules under real operating conditions. Solar Energy, 184: 292–304.

Maren, IB., Bello, AA., Dandakouta, H. and Elijah, R. I. 2022. Performance Evaluation of Some Selected Wind Turbines in Heipang Wind Speed Regime. Nigerian Journal of Tropical Engineering, 16(1): 1590–1597.

Nacar, M., Özer, E. and Yılmaz, AE. 2021. A Six Parameter Single Diode Model for Photovoltaic Modules. Journal of Solar Energy Engineering, 143(1): 1-20.

Naggarapu, M., Shakeera, S. and Venkataraman, H. 2023. Battery Modelling and Performance Analysis of Time-Varying Load Using Simulink. 11th International Symposium on Electronic Systems Devices and Computing (ESDC). held in Sri City, India, 04-06 May 2023, pp. 1-5.

Oyedepo, SO. 2012. Energy and Sustainable Development in Nigeria: The Way Forward. Energy Sustainable Society, 2(15): 1-17. https://doi.org/10.1186/2192-0567-2-15.

Hassan, Q., Algburi, S., Sameen, A., Alman, HM. and Jaszczur, M. 2023. A review of hybrid renewable energy systems: Solar and wind-powered solutions: Challenges, opportunities, and policy implications, Results in Engineering, 20: 1-25.

Rehman, S., Natrajan, N., Mohandes, M., Alhems, L. M., Himri, Y. and Allouhi, A. 2020. Feasibility Study of Hybrid Power Systems for Remote Dwellings in Tamil Nadu, India. IEEE Access, 8: 143881–143890.

Saha, G., Bhadra, M. and Sen, T. 2023. Simulation and Modeling of PV and Wind Hybrid Power System. International Journal for Multidisciplinary Research, 5(3), 1–9. https://doi.org/10.36948/ijfmr.2023.v05i03.3719

Sawant, S., Yarramsetty, C., Moger, T. and Jena, D. 2023. Role of Battery Energy Storage in Enhancing the Reliability of Wind-Integrated Power Systems. 2023 IEEE IAS Global Conference on Emerging Technologies (GlobConET). held in London, United Kingdom, 19-21 May 2023, pp. 1-6

Seo, S., Oh, S-D. and Kwak, H-Y. 2019. Wind turbine power curve modeling using maximum likelihood estimation method. Renewable Energy, 136: 1164–1169.

Corresponding author's e-mail address: eni-ikeh.stella@mouau.edu.ng

Shabani, M., Dahlquist, E., Wallin, F. and Yan, J. 2021. Techno-economic impacts of battery performance models and control strategies on optimal design of a grid-connected PV system. Energy Conversion and Management, 245: 1-21.

Sigarchian, SG., Malmquist, A. and Fransson, T. 2014. Modeling and Control Strategy of a Hybrid PV/Wind/Engine/Battery System to Provide Electricity and Drinkable Water for Remote Applications. Energy Procedia, 57: 1401–1410.

Teyabeen, AA., Akkari, FR. and Jwaid, AE. 2018. Power Curve Modelling for Wind Turbines. Proceedings - 2017 UKSim-AMSS 19th International Conference on Modelling and Simulation, UKSim 2017. held in Cambridge, UK, 05-07 April 2017, pp. 179-184

Tharani, KL. and Dahiya, R. 2018. Choice of battery energy storage for a hybrid renewable energy system. Turkish Journal of Electrical Engineering and Computer Sciences, 26(2), 666–676.

WUXI Technology. 2019. Solar Street Lights, Solar Garden Lights. http://www.wonderfulonline.en.alibaba.com/ accessed on 19 October, 2020.

NOA Testing Inspection Technology. 2018. Crystalline Silicon Terrestrial Photovoltaic Module Test Report. Report No. NNE 19052110, Shanghai, China.

Zhou, W. 2007. Simulation and Optimum Design of Solar-Wind-Diesel Power System. PhD thesis, Hong Kong Polytechnic University, Hung Hom, Hong Kong.

Corresponding author's e-mail address: mareni@unijos.edu.ng